Wave Attenuation from Living Shorelines: A Parameter Study

Kristine A. Mosuela[1] and Jennifer L. Irish[2]

[1]EIT, S.M.ASCE. Department of Civil and Environmental Engineering, Virginia Tech, Mail Code 0105, 750 Drillfield Drive, 200 Patton Hall, Blacksburg, VA 24061, USA; e-mail: kmosuela@vt.edu
[2]Ph.D. P.E., D.CE, F.ASCE. Department of Civil and Environmental Engineering, Virginia Tech, Mail Code 0105, 750 Drillfield Drive, 221E Patton Hall, Blacksburg, VA 24061, USA; e-mail: jirish@vt.edu

ABSTRACT

Living shorelines, such as oyster reefs and wetlands, are praised for being ecologically robust and recreationally attractive, but their influence on estuarine wave energy is less widely understood. Energy dissipation from living shorelines varies depending on the spread, position, and individual characteristics of the living shoreline feature. Furthermore, the efficacy of the feature in attenuating waves is impacted by the wave environment. In this study, these natural features were simulated as bottom friction in the spectral wave model Simulating WAves Nearshore (SWAN) in order to broadly explore the effects of these varying parameters. Results of the study showed that wave environments with larger wave heights and larger periods produced the greatest cumulative energy dissipation and greatest percent wave height reduction. The effectiveness of these nature-based frictional features were prominently limited by water depth. The context of various wave environments in relation to various frictional feature geometries may be useful in designing cost-effective living shorelines.

INTRODUCTION

Shoreline erosion and inshore damage during extreme coastal events relates closely to the wave climate interacting with the shoreline. Sanford and Gao concluded that high onshore wave power is the dominant predictor for shoreline erosion in the Chesapeake Bay (Sanford and Gao 2018). In addition, it is commonly understood that sea level rise further exacerbates shoreline loss (e.g. Dean and Dalrymple 2002). In recent decades, nature-based coastal defenses have thus been increasingly explored as a cost-effective, potentially self-sustaining complement to traditional hardened gray infrastructure (e.g. Borsje 2011, Narayan 2016). Studies show that under certain future conditions including gradual sea level rise, natural features such as saltmarsh and oyster reefs may even be able to adapt to rising sea levels (e.g. Rodriguez 2014, Solomon 2014, Kirwan 2016, Best 2018). In this way, they are widely considered a resilient design alternative with both ecological and engineering benefits.

Emergent vegetation such as mangroves most effectively dissipates wave energy (e.g. Quartel 2007, Bao 2011, Moeller 1996), however near-emergent or intertidal features such as saltmarsh grasses and oyster reefs also demonstrate significant attenuating effects on wave energy (e.g. Anderson 2011, Augustin 2011). Although wave attenuation decreases as water depths above the

dissipative natural feature increase, submerged natural features such as submerged aquatic vegetation and coral reefs can in some conditions exert enough drag force to demonstrably reduce wave heights (e.g. Anderson 2011, Hardy 1991, Zhu 2017, Osorio 2017). Greater vegetation density and longer cross-shore widths of these natural frictional features consistently result in greater attenuation (e.g. Anderson 2011). However, although most studies agree that the efficacy of nature-based defenses is limited to lower-energy wave environments (e.g. Submaranian 2006, Swann 2008), the particular effects of wave height and wave period are less conclusive (Anderson 2011). This study attempts to explore the effects of wave environments more systematically: wave characteristics are varied against natural frictional features. The frictional features are configured both as wide, uniform areal spreads as well as narrower strips offset from the shoreline that are more typical of smaller-scale restoration efforts.

METHOD

The effects of wave climate on the efficacy of various types of natural features was explored using a third-generation spectral wave model, Simulating WAves Nearshore (SWAN) (Delft 2017). The basis of the model is the wave action balance equation, and the model is widely used in the types of environments simulated in this study, i.e. coastal regions with shallow water. Boundary conditions and wind may be used to drive the model, and factors including shoaling, refraction, dissipation by bottom friction, white-capping, depth-induced breaking, and non-linear wave-wave interactions are accounted for in wave propagation (Booij 1999).

The simulations represented an idealized coastal region with a straight shoreline and constant bathymetric slope, using the simplest default model configurations: this included stationary time, 2D (i.e. longshore and cross-shore) mode, and water level positioned at the vertical datum. Incident wave conditions were specified at the offshore model boundary, where no wave generation by wind within the modeling domain was considered. Whitecapping, breaking, and friction was turned on while quadruplet wave-wave interactions was turned off. The computational grid domain was a 3000 m by 3000 m rectangular grid with 0.5 m cells in the cross-shore direction and 300 m cells in the longshore direction. Bathymetry was alongshore-uniform, with a constant 0.05 cross-shore slope; offshore boundary depth was 150 m. A unidirectional (onshore) JONSWAP-shaped wave spectrum was applied at the offshore boundary, and the frequency resolution varied as the peak period was varied at the boundary.

Various wave conditions applied to the model. Based on inspection of preliminary simulations, energy dissipation for peak periods less than 5.0 seconds were found to be very low, therefore 5.0 seconds was set as the lower limit for peak period in subsequent analyses. Similar modeling studies for both submerged and emergent natural features also analyze waves with periods up to 20 seconds (i.e. infragravity waves) (e.g. Tang 2017, Horstman 2014); 20 seconds was likewise selected as an upper limit for peak wave period in order to span from deep- to shallow-water wave conditions in the parameter study. In the Chesapeake Bay (Delaware, Maryland, and

Virginia), typically wave periods are 3 to 4 seconds and significant wave heights are less than 2 meters (Lin 2002). Peak wave periods selected for this study were 5.0, 10.0, 15.0, and 20.0 seconds. Small wave period environments, such as those equivalent to boat wakes or wind waves with short fetch distances, were effectively excluded. Selected wave heights at the offshore boundary of the model were 0.5, 1.0 ,1.5, and 2.0 meters.

Aside from the wave environment, the friction environment—representing the natural feature—was the main parameter varied in the simulations. Although SWAN contains a module that "explicitly" computes energy dissipation by vegetation, this was not used in order to more generally represent a range of natural feature types, including reefs. Aside from this module, SWAN contains three "implicit" modes of computing dissipation by bottom friction: JONSWAP (Hasselmann et al. 1973), Collins (Collins 1972), and Madsen (Madsen et al. 1988). Only the Collins and Madsen formulations have the provision to be varied across the domain in SWAN. Therefore, JONSWAP was eliminated as an option. The Madsen formulation can be directly transformed into the more familiar Manning's representation of bottom friction; however, to integrate this into SWAN requires manipulation of the source code. Furthermore, this Manning's-Madsen approach has a demonstrated upper limit that prohibits accurate representation of highly dissipative features; one study found that this limit occurred at around an equivalent Manning's n of 0.055 (Baron-Hyppolite 2019, Nowacki 2017, Smith 2016). Although Baron-Hyppolite and Nowacki may have different conclusions regarding the accuracy of the "explicit" formulation versus "implicit" formulations, the Collins formulation in particular has been shown by Nowacki to have good spectral performance (Baron-Hyppolite 2019, Nowacki 2017). For these reasons, the Collins formulation was used in this study.

For the control cases, the friction coefficient used for the entire domain was the default 0.015, representing a sandy bottom (Delft 2017). The variable friction cases had a significantly higher Collins bottom friction coefficient: this value was assigned to increasingly wider cross-shore widths or increasingly offset narrow strips, in 10-meter increments starting from the shore out to 300 meters offshore. A depiction of the first three variable friction cases for each of the two types of feature configurations is shown in Figure 1.

Bottom friction is often used as a calibration parameter; therefore, there is ample uncertainty in the empirical equivalents of Collins friction coefficients. In this study, a 0.105 Collins coefficient was used to represent the natural feature; this is seven times higher than the default Collins coefficient for a sandy bottom. In previous studies, 0.006 has been used for a fine silt bottom (Xu 2013) and up to 0.4 was used to represent submerged aquatic vegetation (Nowacki 2017). In a calibration study by Young and Gorman on the Great Australian Bight, the JONSWAP bottom friction coefficient in a similar third-generation spectral wave model was two to four times the default coefficient for a sandy bottom (Young 1993). Although the linearized JONSWAP formulation was decidedly less accurate than the Collins formulation, which has a more nonlinear dependence on spectral energy, the order of magnitude for calibration is a useful reference (Young 1993).

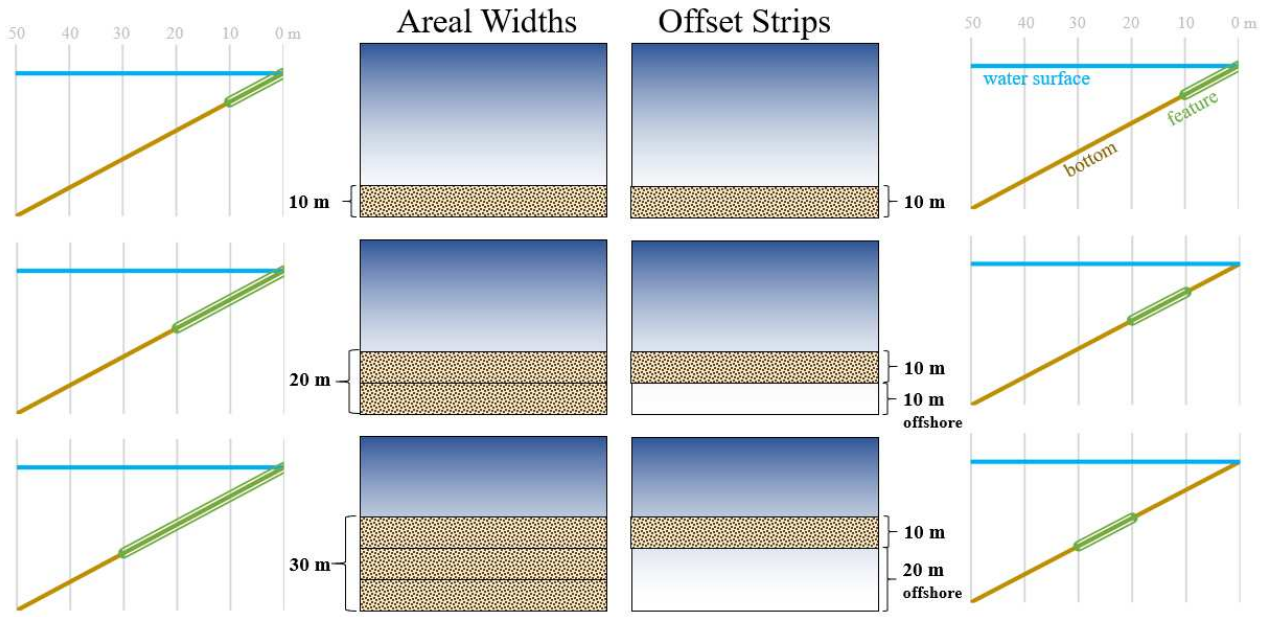

Figure 1: Example of frictional feature configurations up to 30 meters in both the areal width cases (left) and offset strip cases (right). The shoreline corresponds to the bottom of the diagram, while light to dark blue shading indicates respectively shallower to deeper depths.

Likewise, Zhu estimated that the bottom friction coefficient for a coral reef flat is an order of magnitude greater than that for a sandy bottom (Zhu 2004). Therefore, a Collins coefficient that is seven times the default for a sandy bottom was conservatively chosen for the varying friction simulations.

RESULTS

Two main variables were explored in the results: 1) change in cumulative energy dissipation due to bottom friction and 2) change in wave height. The cumulative energy dissipation due to bottom friction over the domain was calculated by $\sum_{0}^{X=x} \partial_x dx$ where ∂_x is the energy dissipation due to bottom friction at position x meters from shore, X is the distance at the offshore boundary, and dx is the computational increment in the cross-shore direction. The change in wave height was observed in two different ways. First, the percent change in wave height was calculated by $\frac{H_c - H}{H_c}$ where $H$is the significant wave height 20 meters offshore (i.e. at 1 m water depth), and H_c is the significant wave height of the control (i.e. no frictional feature) case at the same location. Secondly, the ratio between wave heights with and without the frictional feature ($\frac{H}{H_c}$) was taken and is referred to as relative wave height reduction.

Figure 2 demonstrates the results of two simulations: shown is two different wave environments responding to the same frictional feature over the cross-shore profile. It is important to note that the surf zone shifts based on the wave environment applied to the experimental conditions, and

that the SWAN model does not compute wave runup in the foreshore zone. This has the potential to introduce significant error shoreward of the surf zone.

Overall Trends

Generally, the simulation results showed that both significant wave height and wave period are directly related to the change in cumulative energy dissipation due to bottom friction over the domain and change in significant wave height (Figure 3). The wave with the largest wave height and wave period thus had the greatest percent reduction in wave height: that is, wave heights in the frictional case with the largest feature widths were 12% lower than in the control case.

Areal Widths – Representing Feature Spread

Figure 4 illustrates that greater wave attenuation was observed in cases where the width of the frictional feature was only a fraction of the offshore peak wavelength; this is partly due to the large wavelengths for the conditions where the greatest wave height reductions were observed. Each combination of wave period and height reached a point where additional feature width resulted in diminishing additional wave attenuation, and water depth played a significant role in these diminishing returns.

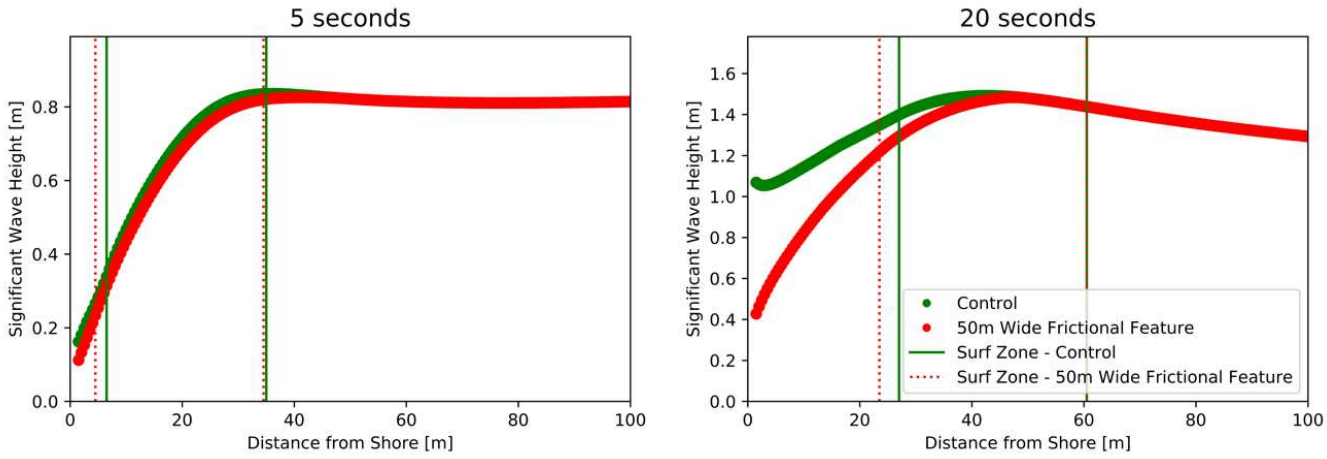

Figure 2: Significant wave heights along a 100 meter transect of a 0.05 uniformly sloped beach for two offshore boundary cases: 5 second peak period and 20 second peak period waves, both with a 1.0 m significant wave height. The control case (i.e. no frictional feature) is shown alongside an example of a single frictional case (i.e. 50 meter areal width).

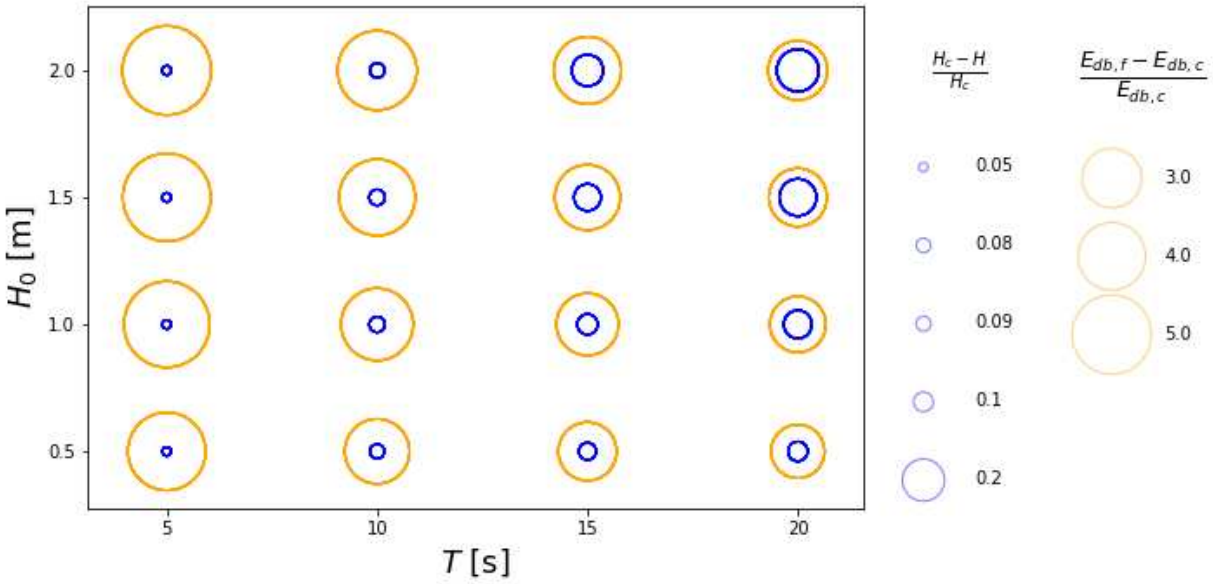

Figure 3: The effect of the offshore boundary wave peak period ($\boldsymbol{H_0}$) and significant wave height (T) are shown for two variables: significant wave height and energy dissipation due to bottom friction. The maximum difference between the control case (H_c and $E_{db,c}$) and areal frictional cases (H and $E_{db,f}$) are shown for each H_0 and T combination for a location 20 m offshore (i.e. at 1.0 m depth for a 0.05 sloping beach). The frictional geometries (i.e. 0.105 Collins friction coefficient) included range from 10 meters to 300 meters areal width from shore.

Figure 5 more intuitively demonstrates the clear inverse relationship between wave attenuation and depth: even when the change in wave height was adjusted against a single unit of frictional feature, attenuation diminished as water depths increased. Therefore, the apparent diminishing returns of dissipation versus feature width is attributable not to the width of the feature but rather the increasing depths as the frictional feature extended in the offshore direction.

In both Figure 4 and 5, there are several points nearshore where there is zero or negative change in wave height. This is partially due to location of the control point, i.e. the control point at 20 m from the shoreline did not experience attenuation from a frictional feature at 10 m. In some cases (e.g. 15 second period) with larger wave heights, wave heights increased just offshore the edge of the frictional feature compared with the control condition. These cases may also be a result of the difference in surf zone locations for varying offshore peak periods: as the model does not account for run-up, wave heights after the majority of waves have broken may contain more error (i.e. longer wavelengths would be most affected at the control point location).

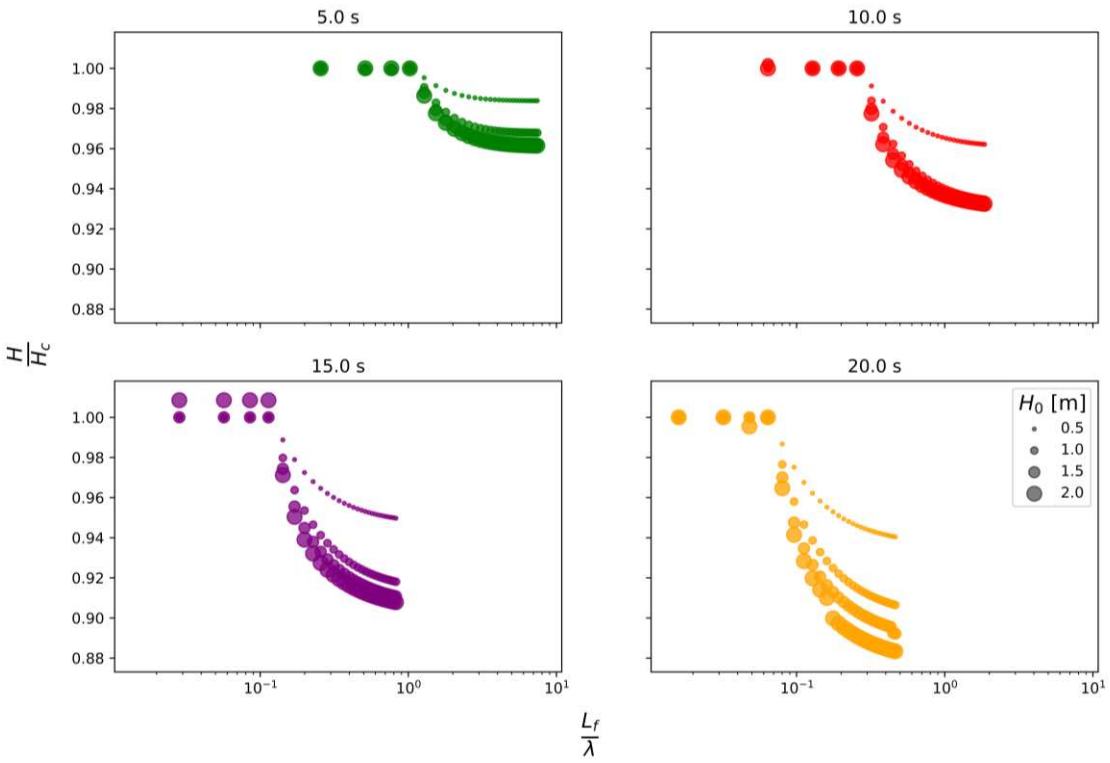

Figure 4: Relative significant wave height reduction ($\frac{H}{H_c}$), where H denotes wave height with the frictional feature present and H_c denotes wave height in the control case) 20 m offshore (i.e. 1.0 m depth) versus areal feature width (L_f) relative to deep water wavelength (λ). The symbols are scaled by the offshore significant wave height (0.5 m, 1.0 m, 1.5 m, and 2.0 m).

Offset Strips – Representing Feature Position

Figure 6 demonstrates relative wave height reductions for offset frictional feature strips as they are placed further offshore.

The relationship between water depth and wave height reduction in the offset strip case is shown in Figure 7. The trends exhibited here are similar to aforementioned trends: wave environments with larger wave periods and larger wave heights experienced the greatest change in wave height due to the feature. The offset strip cases demonstrate more clearly the phenomena also observed in the areal width cases: that is, the water depth at which the feature strip fails to contribute further energy dissipation was deeper for longer wavelengths.

DISCUSSION AND CONCLUSIONS

Simulation results generally corroborate conclusions made in prior research. Indeed, water depth is the dominant controlling factor in the efficacy of a frictional feature. Although experiments in the last few decades have focused on lower energy environments, the results of this systematic analysis supports the notion that nature-based defenses in higher energy environments may be a worthwhile pursuit where longer-period waves are expected. Anderson suggested that the dearth

of experiments in higher energy wave environments may be due to questionable durability of the natural feature against more extreme events (Anderson 2011). Therefore, the energy dissipation afforded by the natural features simulated in this study should not be considered in isolation. Indeed, engineered structures such as artificial mangroves, reef balls, and living breakwaters may simplify some of these ecological concerns but does not eliminate them.

Further Research

As mentioned before, one of the most outstanding uncertainties in this study is the Collins bottom friction coefficient. The values for which the Collins friction coefficient has been applied in previous studies spans almost two orders of magnitude (e.g. Xu 2013, Nowacki 2017): it proves to not be subject to the same mathematical constraints as the Madsen-Manning's formulation, but this opportunity has not been fully exploited. That is, there would be great value in further studies coupling field or laboratory data to equivalent model simulations.

The author plans to further iterate on this particular parameter study by including variations in water depths, feature friction, and bed slope. More advanced modeling might also include variations in wind forcing, irregular bathymetry, or wave angle. Indeed, this study is effectively a 1D horizontal implementation, but the 2D horizontal capabilities of SWAN might be more fully employed with more advanced modeling inputs.

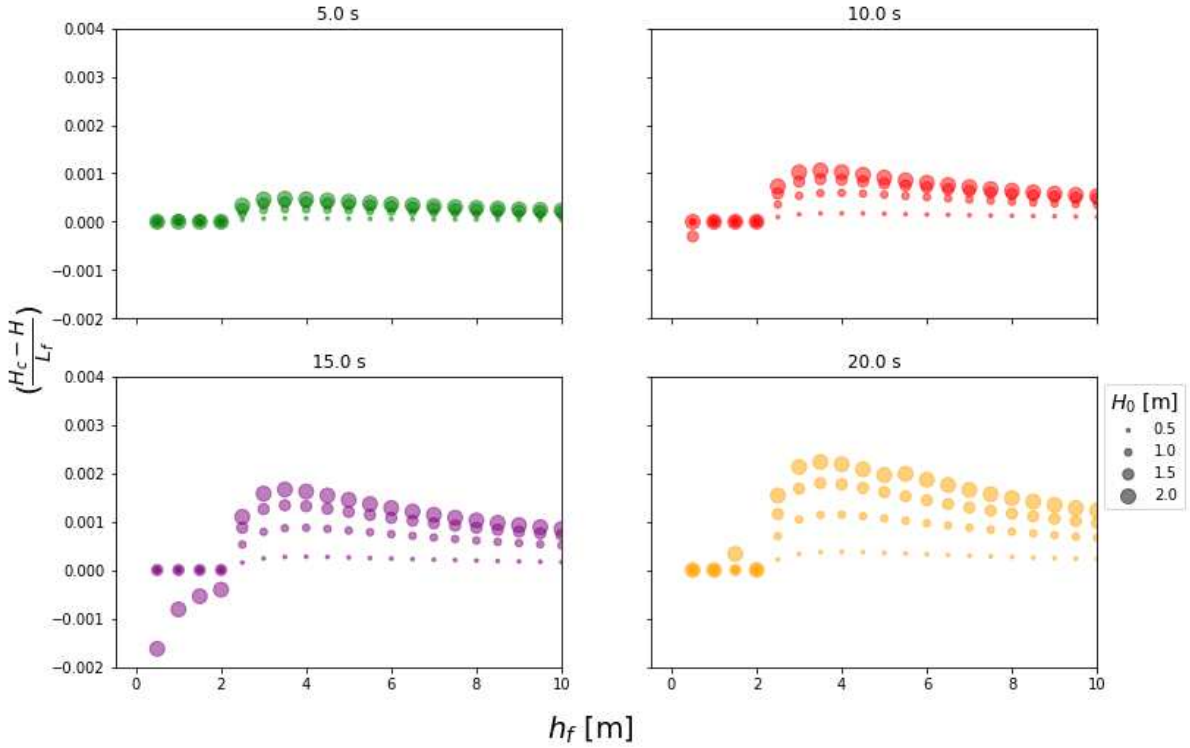

Figure 5: The net change in wave height (H_c-H) per meter width of the feature (L_f) versus water depth (h_f) at the furthest extent of the feature. Symbols are scaled by offshore significant wave height.

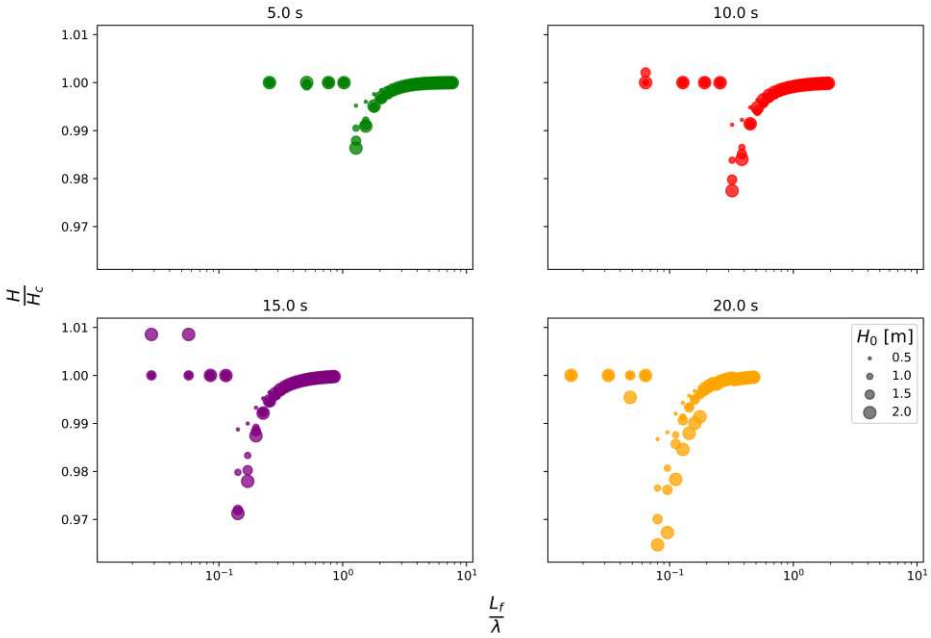

Figure 6: Relative wave height reduction ($\frac{H}{H_c}$) versus offset distance of the 10 m frictional feature from shore (L_f) relative to deep water wavelength (λ). Frictional feature strips are offset every 10 m, starting from shore out to 300 m offshore. Symbols are scaled by offshore significant wave height.

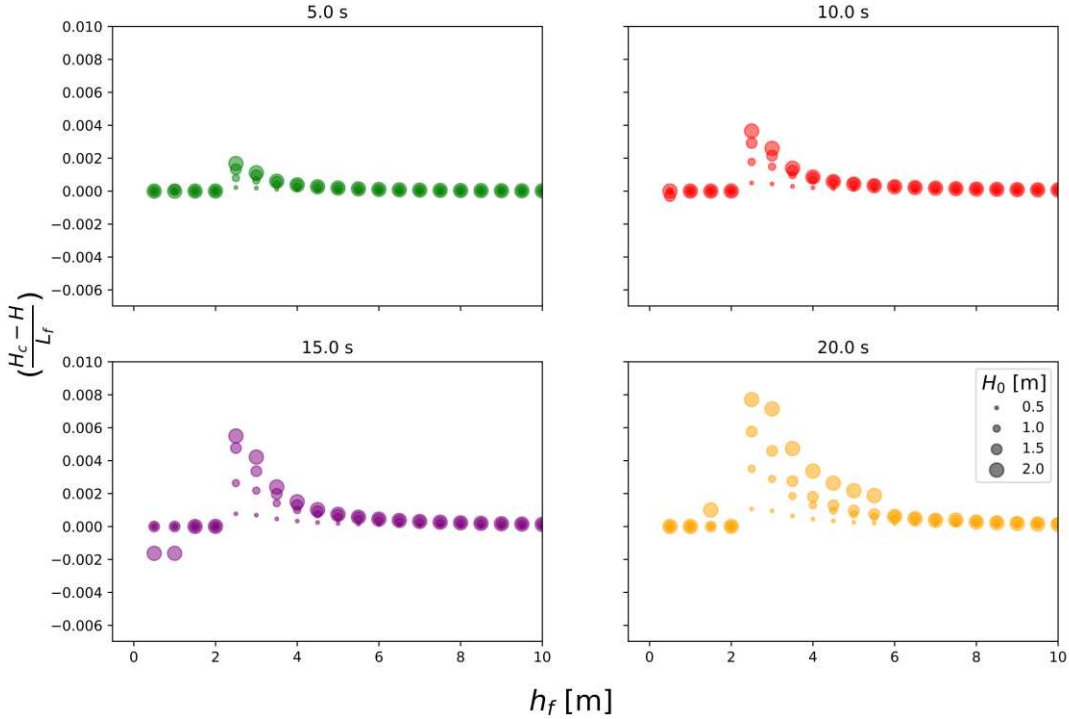

Figure 7: The net change in wave height (H_c-H) per meter width of the feature (L_f) versus water depth (h_f) at the furthest extent of the feature. For example, a 10 m wide offset strip starting from 20 m to 30 m offshore has a h_f of 1.5 m for a 0.05 uniform bed slope. Symbols are scaled by offshore significant wave height.

Applications

After Hurricane Sandy hit the eastern United States, $787 million was allocated by the Department of the Interior for disaster recovery and mitigation (U.S. Department of Interior 2020). this included funding for restoring and strengthening natural features at the shoreline. Systematic studies like these can be used to roughly assess the hydraulic cost-effectiveness of a proposed restoration effort. Before investing in expensive detailed analyses, these "back of the napkin" valuations can be used in tandem with habitat suitability analyses to determine overall project feasibility.

REFERENCES

Anderson, M.E., Smith, J.M., and McKay, S.K. (2011). "Wave Dissipation by Vegetation." U.S. Army Corps of Engineers. ERDC/CHL CHETN-I-82.

Augustin, L.N., Irish, J.L., and Lynett, P. (2009). "Laboratory and numerical studies of wave damping by emergent and near-emergent wetland vegetation." *Coastal Engineering*, 56(2009), 332-340.

Bao, T.Q. (2011). "Effect of mangrove forest structures on wave attenuation in coastal Vietnam." *Oceanologia,* 53(3), 807-818.

Baron-Hyppolite, C. Lashley, C.H., Garzon, J., Miesse, T., Ferreira, C., and Bricker, J.D. (2019). "Comparison of Implicit and Explicit Vegetation Representations in SWAN Hindcasting Wave Dissipation by Coastal Wetlands in Chesapeake Bay." *Geosciences,* 2019(9,8).

Best, U.S.N., Van der Wegen, M., Dijkstra, J., Willemsen, P.W.J.M., Borsje, B.W., and Roelvink, D.J.A. (2018). "Do salt marshes survive sea level rise? Modelling wave action, morphodynamics and vegetation dynamics." *Environmental Modelling and Software*, 109(2018), 152-166.

Booij, N., Ris, R.C., and Holthuijsen, L.H. "A third-generation wave model for coastal regions." *Journal of Geophysical Research,* 104(C4), 7649-7666.

Borsje, B.W., van Wesenbeeck, B.K., Dekker, F., Paalvast, P., Bouma, T.J., van Katwijk, M.M., and de Vries, M.B. (2011). "How ecological engineering can serve in coastal protection." *Ecological Engineering*, 37, 113-122.

Collins, J.I. (1972). "Prediction of Shallow-Water Spectra." *Journal of Geophysical Research,* 77(15), 2693-2706.

Dean, R.G., and Dalrymple, R.A. (2002). *Coastal Processes with Engineering Applications.* Cambridge University Press, Cambridge UK.

Delft University of Technology. (2017). "SWAN User Manual." *SWAN Cycle III version 41.10AB.*

Hardy, T.A., Young, I.R., Nelson, R.C., and Gourlay, M.R. (1991). "Wave Attenuation on an Offshore Coral Reef." *Proc., International Coastal Engineering Conference,* 1(1991), 330-344.

Hasselmann, K., Barnett, T.P., Bouws, E., Carlson, H., Cartwright, D.E., Enke, K., Ewing, J.A., Gienapp, H., Hasselmann, D.E., Kruseman, P., Meerburg, A., Müller, P., Olbers, D.J., Richter, K., Sell, W., and Walden, H. (1973). "Measurements of wind-wave growth and swell decay during the Joint North Sea Wave Project (JONSWAP)." *Deutches Hydrographisches Institut: Ergänzungsheft 8-12.*

Horstman, E.M., Dohmen-Janssen, C.M., Narra, P.M.F., van den Berg, N.J.F., Siemerink, M., and Hulscher, S.J.M.H. (2014). "Wave attenuation in mangroves: A quantitative approach to field observations." *Coastal Engineering,* 94(2014), 47-62.

Lin, W. Sanford, L.P., and Suttles, S.E. (2002). "Wave measurement and modeling in Chesapeake Bay." *Continental Shelf Research,* 22(2002), 2673-2686.

Kirwan, M.L., Temmerman, S., Skeehan, E.E., Guntenspergen, and G.R., Fagherazzi, S. (2016). "Overestimation of marsh vulnerability to sea level rise." *Nature Climate Change,* 6 (March 2016).

Madsen, O.S., Poon, Y.K., and Graber, H.C. (1988). "Spectral Wave Attenuation by Bottom Friction: Theory." *Coastal Engineering,* 1988, 492-504.

Moeller, I., Spencert, T. and French, J.R. (1996). "Wind Wave Attenuation over Saltmarsh Surfaces: Preliminary Results from Norfolk, England." *Journal of Coastal Research,* 12(4), 1009-1016.

Narayan, S., Beck, M.W., Reguero, B.G., Losada, I.J., van Wesenbeeck, B., Pontee, N., Sanchirico, J.N., Ingram, J.C., Lange, G., and Burks-Copes, K.A. (2016). "The

Effectiveness, Costs and Coastal Protection Benefits of Natural and Nature-Based Defences." *PLoS ONE*, 11(5).

Nowacki, D.J., Beudin, A., and Ganju, N.K. (2017). "Spectral wave dissipation by submerged aquatic vegetation in a backbarrier estuary." *Limnol. Oceanogr*. 62(2017), 736–753.

Osorio-Cano, J.D. Osorio, A.F., Pelaez-Zapata D.S. (2017). "Ecosystem management tools to study natural habitats as wavedamping structures and coastal protection mechanisms." *Ecological Engineering,* 2017.

Quartel, S. Kroon, A., Augustinus, P.G.E.F., Van Santen, P., and Tri, N.H. (2007). "Wave attenuation in coastal mangroves in the Red River Delta, Vietnam." *Journal of Asian Earth Sciences*, 29(2007), 576-584.

Rodriguez, A.B., Fodrie, F.J., Ridge, J.T., Lindquist, N.L., Theuerkauf, E.J., Coleman, S.E., Grabowski, J.H., Brodeur, M.C., Gittman, R.K., Keller, D.A., and Kenworthy, M.D. (2014). "Oyster reefs can outpace sea-level rise." *Nature Climate Change,* 4 (June 2014).

Sanford, L.P. and Gao, J. (2018). "Influences of Wave Climate and Sea Level on Shoreline Erosion Rates in the Maryland Chesapeake Bay." *Estuaries and Coasts*, 41(Suppl 1), S19-S37.

Solomon, J.A, Donnelly, J.A., Melinda, J. and Walterst, L.J. (2014). "Effects of Sea Level Rise on the Intertidal Oyster Crassostrea Virginica by Field Experiments." *Journal of Coastal Research,* 68(sp1), 57-64.

Subramanian, B., Martinez, J., Luscher, A.E., and Wilson, D. (2006). "Living Shoreline Projects in the Past 20 Years." *Management, Policy, Science, and Engineering of Nonstructural Erosion Control in the Chespeake Bay: Proc., 2006 Living Shoreline Summit.* CRC Publ. No. 08-164.

Swann, L. (2008). "The Use of Living Shorelines to Mitigate the Effects of Storm Events on Dauphin Island, Alabama, USA." *Proc., American Fisheries Society Symposium 64:000-000.* American Fisheries Society.

Tang, J., Shen, Y., Causon, D.M., Qian, L., and Mingham, C.G. (2017). "Numerical study of periodic long wave run-up on a rigid vegetation sloping beach." *Coastal Engineering,* 121(2017), 158-166.

U.S. Department of Interior. (2020). "Hurricane Sandy Recovery | U.S. Department of Interior". < https://www.doi.gov/hurricanesandy> (Feb. 15, 2020).

Xu, F., Perrie, W. and Solomon, S. (2013). "Shallow Water Dissipation Processes for Wind Waves off the Mackenzie Delta." *Atmosphere-Ocean,* 51(3), 296-308.

Young, I.R. (1989). "Wave Transformation Over Coral Reefs." *Journal of Geophysical Research,* 94(C7), 9779-9789.

Zhu, L., Li M., Zhang H., and Sui S. (2004). "Wave Attenuation and Friction Coefficient on the Coral-Reef Flat." *China Ocean Engineering,* 18(1), 129-136.

Zhu, L. and Chen, Q. (2017). "Attenuation of Nonlinear Waves by Rigid Vegetation: Comparison of Different Wave Theories." *J. Waterway, Port, Coastal, Ocean Eng.,* 143(5), 04017029-1-12.